River network delineation from Sentinel-1 SAR data

Christopher B. Obida[1], George A. Blackburn, James D. Whyatt and Kirk T. Semple

Lancaster Environment Centre, Lancaster University, Lancaster, United Kingdom LA1 4YQ

*Corresponding author.
E-mail address: c.obida@lancaster.ac.uk (C.B. Obida).

Highlights

- River network data are absent or out of date in most developing countries
- Sentinel-1 data used here to generate high resolution river map
- Sentinel-1 river product superior to alternative remotely-sensed sources
- Topologically structured geometric river network supports flow routing
- Technique can provide essential river network data for many countries

Abstract

In many regions of the world, especially in developing countries, river network data are outdated or completely absent, yet such information is critical for supporting important functions such as flood mitigation efforts, land use and transportation planning, and the management of water resources. In this study a new method was developed for delineating river networks using Sentinel-1 imagery. Unsupervised classification was applied to multi-temporal Sentinel-1 data to discriminate water bodies from other land cover types then the outputs were combined to generate a single persistent water bodies product. A thinning algorithm was then used to delineate river centre lines which were converted into vector features and built into a topologically structured geometric network. The complex river system of the Niger Delta was used to compare the performance of the Sentinel-based method against alternative freely available waterbody products from USGS, ESA and OpenStreetMap and a river network derived from a SRTM DEM. From both raster-based and vector-based accuracy assessments it was found that the Sentinel-based river network products were superior to the comparator data sets by a substantial margin. The resulting geometric river network was used to perform flow routing analysis which is important for a variety of environmental management and planning applications. The approach developed in this study holds considerable potential for generating up to date, detailed river network data for the many countries globally where such data are deficient.

Key words

Sentinel-1, image processing, river delineation, large scale mapping, data comparison, geometric network

1. Introduction

Rivers are important resources that sustain a substantial proportion of the world's population, through the vital ecosystems services they provide (Zeng et al., 2015). Determining the spatial and temporal dynamics of surface waters remains challenging (Khandelwal et al., 2017). Globally, there has been increased need for monitoring natural water resources in response to changing climate and pollution from anthropogenic sources (Haddeland et al., 2014). Resource managers need efficient ways of monitoring water, determining flow regimes, extent and discharge. Modellers and scientist alike need hydrological information for forecasting extreme events such as floods, and accurate river network data to model the fate of pollutants in rivers globally (Garneau et al., 2017; Zeng et al., 2015). However, detailed maps of river networks do not exist for many developing countries and even where previous surveys have taken place they are often significantly out of date, especially for dynamic systems such as deltas.

Remote sensing offers a low-cost and efficient alternative to ground-based surveys for river network delineation, particularly in light of recent improvements in the temporal and spatial resolution of satellite data, e.g. using frequent acquisitions from MODIS (Khandelwal et al., 2017). Optical remote sensing has been widely used for river network delineation using a range of automatic and semi-automatic techniques (Isikdogan et al., 2017). For example, Landsat data was used to delineate complex braided network of the Brahmaputra river which flows through China, India and Bangladesh and a tidal river network in Berau Bay, New Guinea (Yang et al., 2014). The study revealed that spectral mixture within pixels resulting from the spatial resolution of the imagery resulted in commission and omission errors in river classification. Others have noted that this approach is not suitable for smaller rivers (Domeneghetti et al., 2014; Ogilvie et al., 2015). Allen and Pavelsky (2015) developed NAR-Width (North American River Width) which uses Landsat data in a software suite called RivWidth to delineate and estimate the width of rivers in North America. However, the model is largely restricted to North America, due to the input data and some aspects of the algorithm that prevents it use in other global regions.

Water body extraction from optical imagery has also been achieved using other approaches. These include region growth and edge detection, and water indices such as the Normalised Difference Water Index (NDWI) (Isikdogan et al., 2017; Zeng et al., 2015), Modified Normalised Difference Water index (MNDWI) (Ogilvie et al., 2015; Yang et al., 2014), Automated Water Extraction Index (AWEI) (Feyisa et al., 2014), and Land Surface Water Index (LSWI) (Ogilvie et al., 2015). Isikdogan et al. (2017) introduced the RivaMap mapping engine which is based on Landsat data and was used to delineate rivers at a continental scale (North America). However, the output of RivaMap is an unstructured vector network, which can limit its applicability in studies of hydrological flows. Furthermore, all of the methods that are applied to optical data such as MODIS and Landsat, can be limited by cloud cover, which restricts useable repeat image acquisitions and limits the ability to detect the persistence or dynamics of surface water bodies.

Digital Elevation Models (DEMs) derived from different satellite missions have been widely used for hydraulic studies, hydrologic modelling and river network delineation (Gülgen, 2017; Kumar et al., 2017). Commonly used DEMs include the Shuttle Radar Topographic Mission (SRTM) 1 arc second, SRTM 3 arc second and Advanced Spaceborne Thermal Emission and Reflection Radiometer (ASTER) 30m products (Vimal et al., 2012). Algorithms for river network delineation such as the hydrological tools in ArcGIS version 10, Arc Hydro (Kim et al., 2015), TauDEM (Castronova and Goodall, 2014), HydroSHEDS (Lehner et al., 2008) and GWD-LR (Yamazaki, 2014) all use DEMs as input data (Khan et al., 2014). This approach is popular because important hydrological parameters such as river length, area, slope, flow direction, accumulation, aspect and watershed area can be extracted from DEMs. However, because these methods use the direction of steepest decent for delineation, this can lead to over estimation of river network elements in lowland and delta environments (Gülgen, 2017; Isikdogan et al., 2017; Vimal et al., 2012). Rahman, et al (2010) demonstrated in a study of the delta region of Bangladesh that errors were proportional to degree of flatness. In addition, some researchers have highlighted the inaccuracies of using DEMs for river delineation such as the inability of the algorithms to consider manmade features (Kumar et al., 2017). DEMs can also contain erroneous changes in elevation in some areas, referred to as sinks, which result in computational errors in flow direction and ambiguity in alignment of the delineated river network (Kumar et al., 2017).

Airborne Light Detection and Ranging (LiDAR) has been applied in stream network delineation (Maderal et al., 2016). LiDAR data provides height information that has been used to characterise catchments, generate flow direction and delineate rivers in wide range of landscapes (Li & Wong, 2010). Wavelet-based filtering techniques, curvature analysis, and geodesic operations have all been previously applied to LiDAR data for stream delineation (Cho et al., 2011; Lashermes et al., 2007; Passalacqua et al., 2012). However, airborne LiDAR data capture is expensive, spatially limited in application and requires significant time to process the large point cloud (Hamada et al., 2016). Hence, for the scale of whole fluvial systems, the costs associated with the use of LiDAR can be prohibitive, especially in developing countries.

Citizen science initiatives such as OpenStreetMap (OSM) also constitute a genuine source of digital geographic data (Haklay, 2010). Such web mapping systems offer a step change in the availability of important geographic data such as river networks. As a result, data is now accessible in a searchable and usable format, and the data quality can be as good as that of national mapping agencies (Haklay, 2010). However, the quality of data from such sources is contingent on the level of participation and the experience and knowledge of the contributors (Haklay, 2010), with lower levels of mapping activity in the Global South (Bittner, 2017;

Graham et al., 2015), particularly in rural areas, with little emphasis on natural features such as rivers.

Given the above limitations in existing techniques and products, new remote sensing methods are needed for repeatedly mapping river networks in a timely fashion, particularly in developing countries. Sentinel-1 SAR C data acquired by the European Space Agency (ESA) has the potential to overcome the identified limitations. The dual satellites (Sentinels 1A and B) launched in 2014 and 2016 offer global coverage (Haas and Ban, 2017; Miranda et al., 2016), with a combined temporal resolution of 5-6 days and spatial resolution of 20m by 5m and ground sampling distance of 10m (Ardhuin et al., 2017; Malenovský et al., 2012; Veloso et al., 2017). Utilizing these data can potentially enhance scientific studies requiring detailed river network delineation in complex environments.

Therefore, the aim of this study was to develop an effective method of delineating river networks using Sentinel-1 data. The objectives were to: (a) investigate the potential of utilizing a time series of Sentinel-1 images for accurate river network delineation; (b) compare Sentinel-1 outputs with existing river network data sets; (c) build a complete topologically structured geometric river network dataset; (d) demonstrate the potential of the network dataset by tracing the movement of pollution from a point source event through the fluvial system.

2. Method

2.1. Study site

The Niger Delta (Figure 1) is the largest river delta in Africa and the third largest in the world (Kadafa, 2012; UNEP, 2011). It occupies an estimated 70,000 km^2 in area and supports a population of 30 million people. Information on the river network in the region is therefore important because this can enable effective monitoring of changes in the distribution of this highly dynamic fluvial system, and the resultant impacts on resources and threats to the population. Since most of the population depend on fishing and river water for domestic activities, detailed information on the river network is vital within the framework of management and monitoring of key resources. Likewise, flooding is a common occurrence in the Niger Delta which can have devastating effects on the population and infrastructure (Ekeu-Wei and Blackburn, 2018; NHSA, 2014). However, there is a paucity of digital spatial data for the Niger Delta, and there is no national spatial data infrastructure (Anifowose et al., 2012; Nwilo and Badejo, 2005). Accurate and up to date data on the river network are now needed to support the development of flood mitigation schemes and appropriate land use strategies. Furthermore, the Niger Delta is the region in which the majority of Nigeria's oil and gas extraction takes place (Anejionu et al., 2015). There is a long and well-documented history of oil pollution incidents in the region, with rivers among the worst affected environments, therefore, river network data are crucial in employing pollution mitigation measures (Obida et al, 2018). In particular, there is a pressing need for a detailed topologically-structured river network dataset for use in modelling the dispersion and fate of crude oil in the Niger Delta and its impact on the environment and human health.

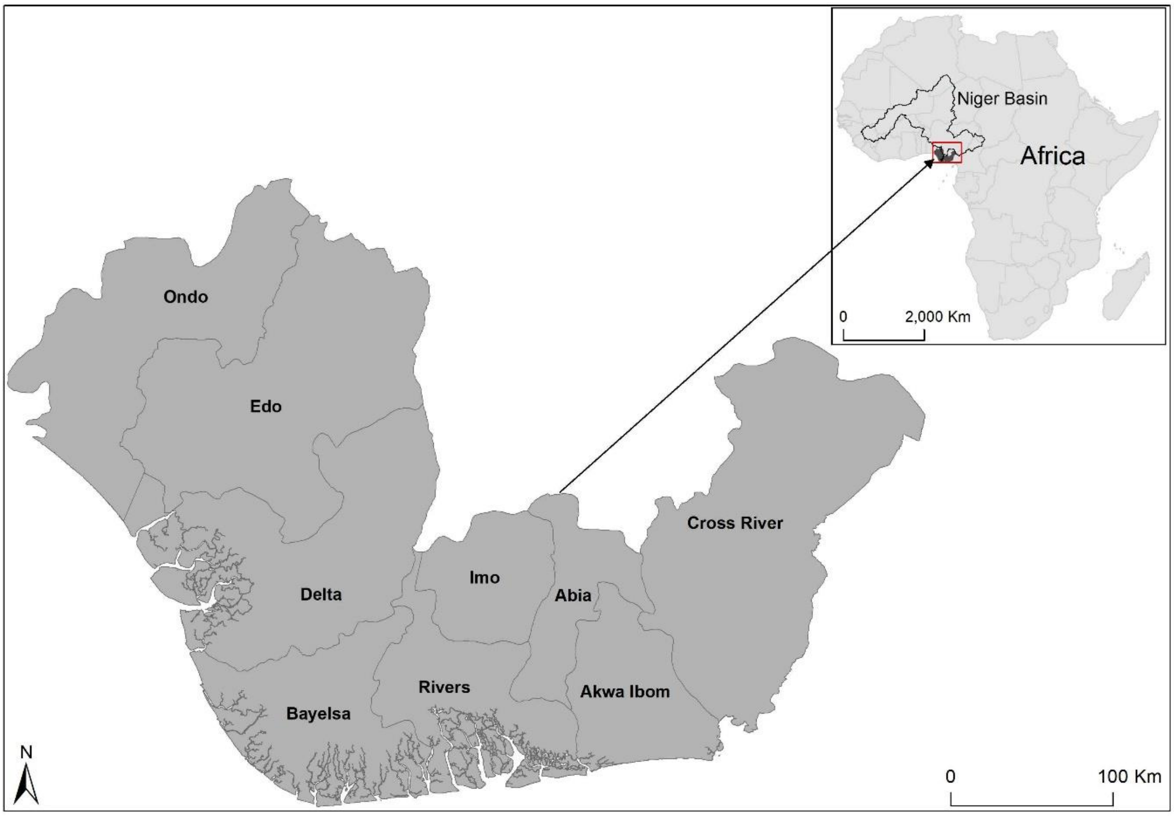

Fig.1. The study area, the Niger Delta. Inset map shows the location of the Niger Delta in relation the drainage basin that supplies water and sediment to the delta.

2.2 Methodological Framework

In this study, multi-temporal Sentinel-1 SAR C were used for both raster-based and vector-based river channel delineation. Raster channels were delineated using classification techniques and thinning algorithms were applied to generate vector data. Both the raster and vector river delineations from Sentinel-1 were compared to existing river data products by performing accuracy assessments relative to reference river channel data. Network topology and attribution were then added to the Sentinel-derived rivers to allow more complex network analysis. The methodological framework is shown in Figure 2.

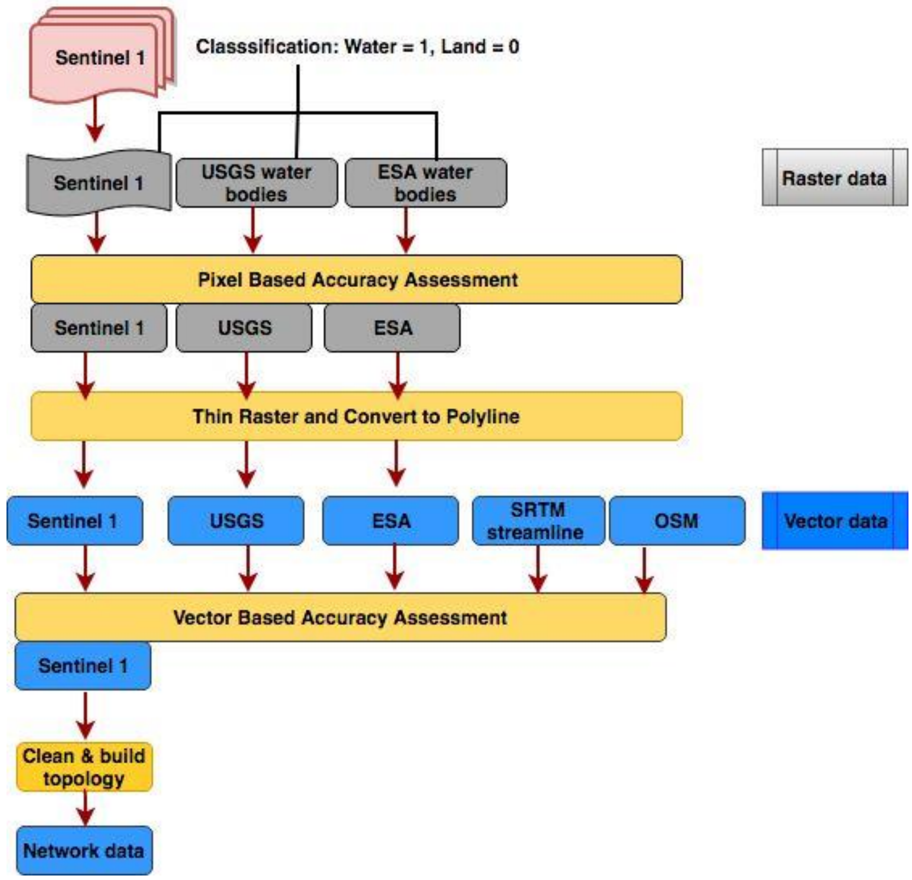

Fig.2. Methodological framework for accuracy assessment and river network extraction based on the different data sources.

2.3. Source Data

2.3.1 Sentinel-1 data

The Sentinel-1 data were sourced free of charge from the ESA Copernicus Open Access Hub. Here we used the Interferometric Wide swath mode data, the predefined mode for overland applications. The Level-1 Ground Range Detected product type was used, which has been detected, multi-looked and projected to ground range using an Earth ellipsoid model (Veloso et al., 2017). We used the co-polarised VV data because noise restricts the use of VH data as water has a lower radar-cross section in cross polarization than in co-polarized channels (HH or VV) (Bolanos et al., 2016). Dual polarised HH+HV was not available for the study area.

The data have a spatial resolution of 5m by 20m with a ground sampling distance of 10m (Imperatore et al., 2017).

2.3.2 Comparator data

The Landsat global water bodies product was the result of a collaboration between the United States Geological Survey (USGS) and University of Maryland. This raster dataset represents persistent global surface water bodies over the 2000-2012 time period, and is the highest spatial resolution product available globally. ESA global water cover data derived from Envisat ASAR and MERIS data at 300m resolution over the period 2005-2010 were also used. OpenStreetMap (OSM) vector data were also used for comparative purposes. Finally, a river network that we derived from 1 arc second SRTM data (method described in 2.5.2 below) was also used. The SRTM data are available globally and were sourced from the USGS Earth Explorer platform.

2.4 Raster-based analysis

2.4.1 Sentinel-1 data processing and analysis

Image pre-processing routines were performed in the Sentinel Application Platform (SNAP). Geometric correction was carried out by the initial application of orbital files to correct orbit vectors (Zhang et al., 2016). Range-Doppler Terrain Correction was applied to each image for accurate geocoding, using the 3 arc second SRTM DEM, thus accounting for variations in local elevations (Veloso et al., 2017). Multi-temporal image co-registration was then carried out, since the study involved application of multi-temporal data, consisting of the 14 images available for the study site acquired between May 2015 and January 2017, using the first available image as the master (Sowter et al., 2016). Radiometric correction was applied to the images by calibrating the data to sigma nought, which is the backscatter coefficient (Misra and

Balaji, 2017). To reduce speckle in the SAR data, the refined Lee Sigma speckle filter was applied (Fu et al., 2017; Haas and Ban, 2017).

Unsupervised classification was used to distinguish between water and land in the multi-temporal Sentinel-1 data (Ogilvie et al., 2015) as this performed better than supervised classification and thresholding in this context. A K-means unsupervised classification approach was applied to the data in SNAP (Jain, 2010). Since water has a distinctive response in C–band SAR signals, water bodies were partitioned into an output class as a result of the K-means procedure.

Following classification, the outputs were combined into a single image in ArcMap 10.4 with pixel values ranging from 1-14 based on a count of the number of times each pixel was classified as water across the time series of images (Khandelwal et al., 2017). This was to differentiate between persistent and ephemeral water bodies, particularly due to high tides and floods (Rahman & Thakur, 2017). In the combined image, a value of 1 indicates a low probability of the pixel being a persistent water body, while pixels with a value of 14 indicates a high probability of the pixel being a persistent water body. Reference data on the locations of permanent river channels were collected by visual interpretation of ArcGIS World Imagery (Digital Globe GeoEye-1 images from 2013 – 2017 at 0.5m resolution). Using the reference data an optimum threshold was identified for the number of times each pixel was classified as water in order to delineate the river network most effectively. This was determined by incrementally increasing (from 1 to 14) the persistence value required for classifying a pixel as a permanent water body, and for each increment, the output water body map was tested for accuracy against the reference data set. This analysis showed that users' accuracy of the output water body map increased substantially as the required level of persistence increased, up to a value of 12 where it reached a plateau of 89%. Hence, all pixels with persistence values of 12 and above were used to map permanent water bodies in the study area.

2.4.2 Raster-based accuracy assessment

High-resolution Google Imagery, acquired in 2018, was visually evaluated in order to generate reference data (Feyisa et al., 2014). A total of 700 reference points were captured through ‘heads up’ digitizing, 350 of which were located in rivers and 350 in other land cover types. The reference data were then compared to the raster-based river networks generated from the Sentinel-1, USGS and ESA data by computing error matrices. Subsequently, user’s, producer’s, overall accuracies and kappa coefficients were calculated (Felipe De Almeida Furtado et al., 2016; Feyisa et al., 2014).

2.5 Vector-based analysis

2.5.1 River network extraction

Here we firstly applied a raster-based centre line extraction method using the thin tool in the Spatial Analyst extension of ArcGIS 10.4 on the river raster generated from the Sentinel-1, USGS and ESA data sets. Secondly, we applied the raster to polyline tool in ArcGIS to convert the thinned centre pixels to a series of vector lines. The rationale of reducing variable river widths to centre pixels and subsequently to lines is to develop a network model where connectivity is the most important property.

2.5.2 River extraction from the SRTM 1 arc second DEM

Methods of extracting river channels from DEMs are well established and have been applied at a variety of scales (Khan et al., 2014; Kumar et al., 2017; Vimal et al., 2012). Here we used the hydrological toolset in ArcGIS 10.4 to extract the river network from the SRTM 1 arc second DEM.

2.5.3 Vector-based accuracy assessment

An independent river network dataset, covering a river length of 800km within the study site, was captured through ‘heads up’ digitizing of high resolution ArcGIS World Imagery. This generated a vector network of river centre lines for use as reference data. These reference data were then used to assess the accuracy of the vector networks derived from Sentinel-1 and the comparator data. Among the comparator data, the OSM and SRTM-derived network data contained river centre lines which could directly be compared to the reference data. In order to facilitate a vector-based accuracy assessment of the ESA and USGS data, these raster based river networks were thinned and converted to polylines.

The vector river networks derived from Sentinel-1 and comparator data were assessed for data completeness (length) and positional accuracy (overlap) against the manually digitised reference network (Li and Wong, 2010; Hamada et al., 2016). The percentage data completeness was calculated based on the stream orders in the network, from small 1st order streams to larger 3rd order streams. In terms of the positional accuracy, 3 different sample sections of the network were assessed by generating 10m, 20m and 30m buffers around the reference network. The percentage of data from the Sentinel-1 and comparator data networks that fell within each of the buffers was used to measure the spatial overlap with the reference data and thereby indicate positional accuracy (Goodchild & and Hunter, 1997).

2.5.4 Building river network topology and attributes

Most river networks derived from remote sensing are devoid of topological properties and connectivity rules such as edges and junctions, meaning that connectivity, flow direction, and flow rate cannot be derived. Building a geometric river network is important to enable its use in a range of applications, including hydrological modelling (Jiang, 2011). Based on the results of the vector-based accuracy assessment the Sentinel-1 river centre line product was selected for building a geometric river network. Initially, the network was cleaned in ArcMap by closing gaps to ensure network connectivity. Gaps <20m were automatically closed by the software, with the few remaining larger gaps being closed manually to ensure complete connectivity. Consequently, the ArcGIS geometric network toolbox was used to build a topologically structured network. In a manually digitised network the flow direction is determined by the direction of digitization as recorded by the software. However, since our network was generated from image data there was no direction of digitization, hence, we used the 'set flow direction' tool in ArcGIS's geometric network toolbox.

2.5.5 Application of the river network for tracing the movement of a point source pollution event

To demonstrate the potential utility of the delineated river network and the attributed topology parameters such as network connectivity and flow direction, an example application was performed. This involves using the geometric network analysis tool to trace the potential pathway of oil released from a spill which enters the river network and moves downstream. We used the example of a known event which occurred on 20th April 2012, where 19,350 litres of crude oil were spilt from a sabotaged 24-inch pipeline in the Nembe LGA of Bayelsa state. The location of this event was recorded in a database maintained by the Nigerian National Oil Spill Detection and Response Agency (https://oilspillmonitor.ng/).

3. Results

3.1 Raster-based Analysis

3.1.1 Raster river network derived from Sentinel-1

Figure 3 shows the binary land cover classifications of the 14 Sentinel-1 images covering the period May 2015 to January 2017. The images show a high degree of visual similarity, but there are differences, especially in the southern part of the study area, which are attributable to the different prevailing hydrological conditions (e.g. river discharge or tidal state) at the time of image capture. The k-means unsupervised classification appears to effectively distinguish between water and other land cover types.

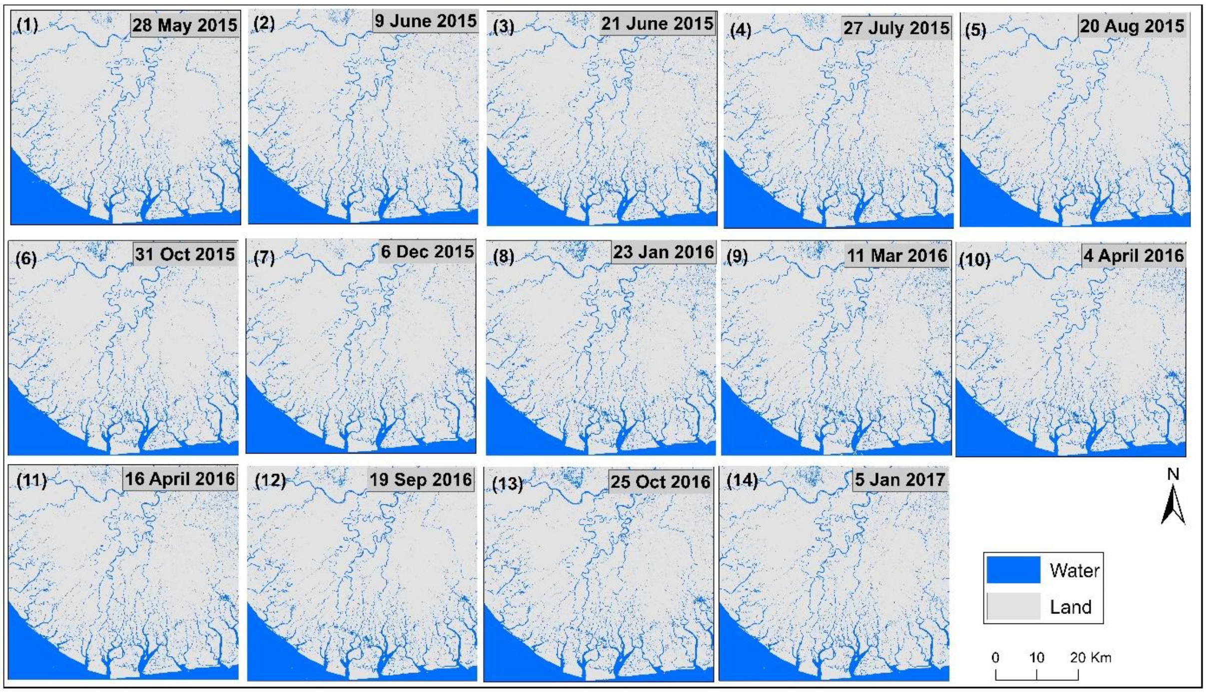

Fig.3. Binary land cover classifications of the Sentinel-1 image time series.

Figure 4 shows the outputs of the Sentinel-1 time series combined into a single image with each pixel placed into one of three categories based on a count of the number of times the pixel was classified as water (the persistence). Pixels with lower values (i.e. in the 1-11 category) represent ephemeral water bodies, whilst pixels with higher values (12-14 category) denote permanent river channels.

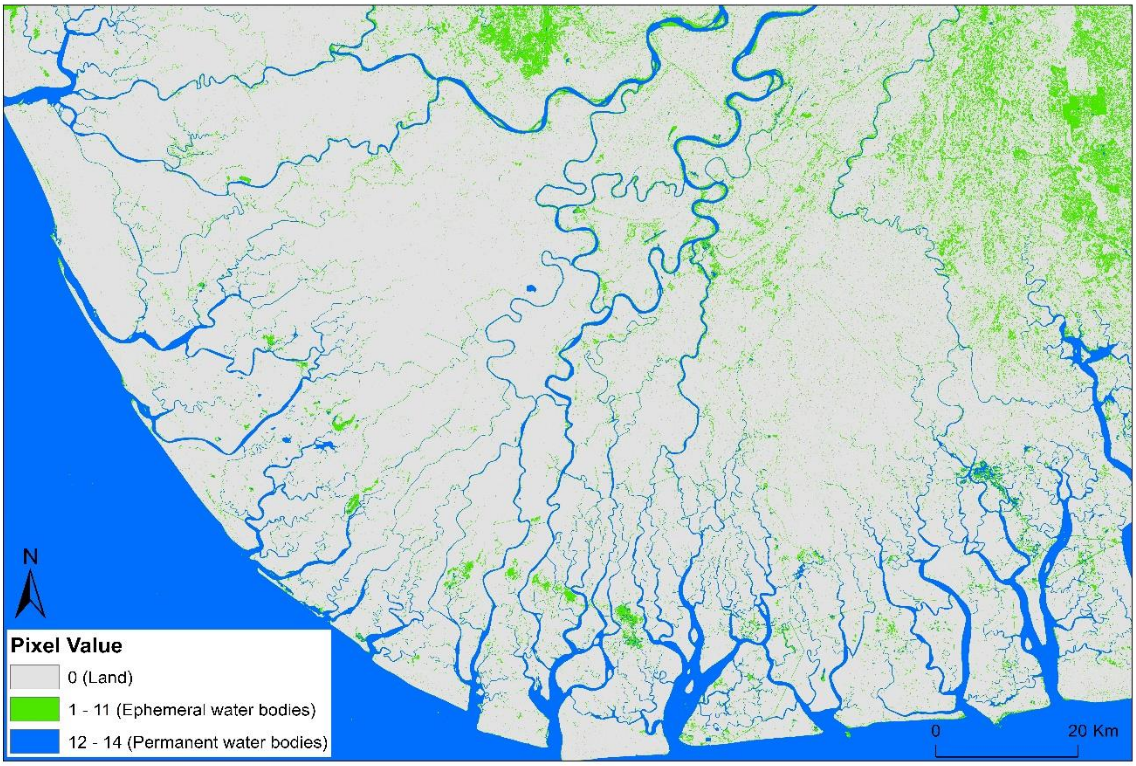

Fig.4. Combined product from the Sentinel-1 time series with each pixel placed into one of three categories based on a count of the number of times the pixel was classified as water.

3.1.2 Raster-based accuracy assessment

Figure 5 shows a comparison of the ESA and USGS water body products with the Sentinel-derived map for a small sample area. It shows the degree to which raster resolution can impact upon river network delineation and potential to further determine the quality of extracted vector data. Table 1 shows the results of the accuracy assessment of the raster-based river networks derived from the Sentinel-1, USGS and ESA data sets. The overall accuracy of the river network derived from Sentinel-1 was much higher than the USGS and ESA products. The user's accuracy for water bodies was consistently higher that than the producer's accuracy which indicated low false positives, across all three data sources. In addition, both the USGS and ESA data had much lower producer's accuracies than the Sentinel-1-derived data which implies an under representation of water in the existing products. USGS and ESA data had low Kappa coefficients while that for the Sentinel-1-derived product was much higher and suggested that classification accuracy was better than random occurrence.

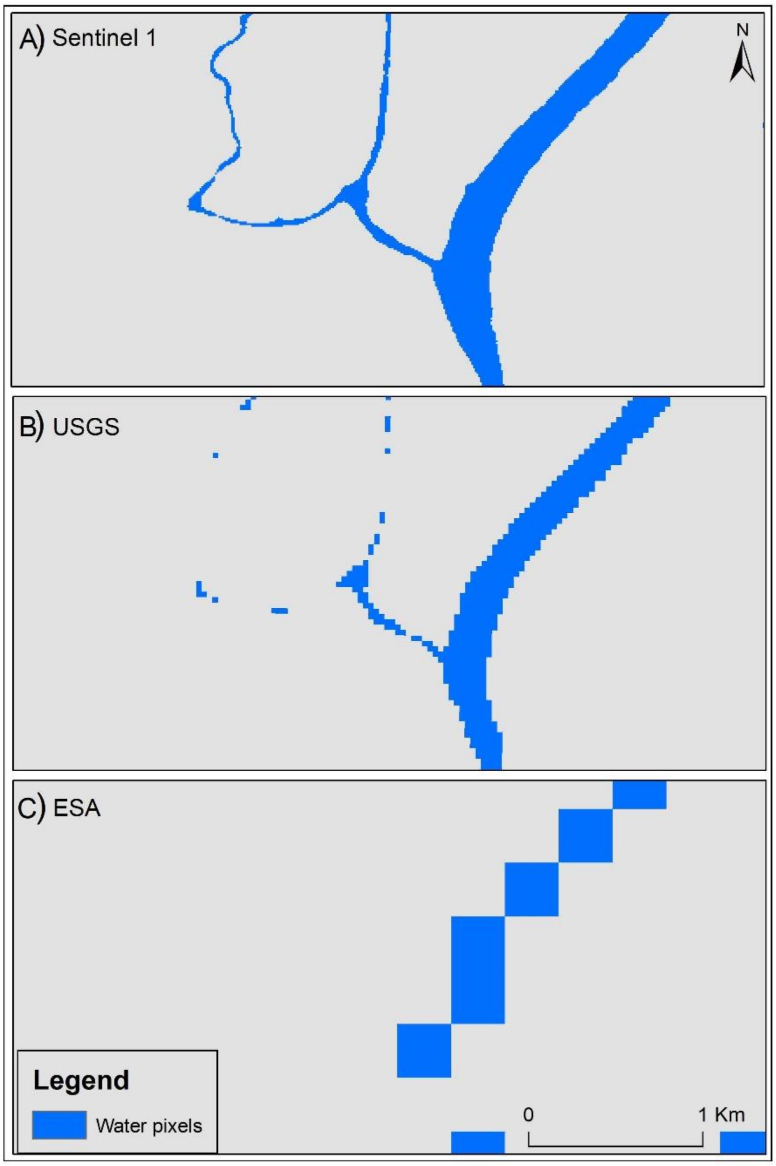

Fig.5. Comparison of extracted raster data sets from: A) Sentinel-1, and comparator data, B) USGS and C) ESA. Blue pixels indicate water.

Table 1

Image based classification accuracies for raster-based river networks derived from Sentinel-1, USGS and ESA data.

Accuracy metric	Sentinel-1	USGS	ESA
Overall accuracy (%)	76	69	60
Producer's accuracy (%)	61	38	21
User's accuracy (%)	89	100	78
Kappa coefficient	0.52	0.38	0.20

3.2 Vector-based analysis

3.2.1 River network extraction from the Sentinel-derived river raster.

Figure 6 shows the effectiveness of the thinning algorithm used to generate the river centreline vector data from the raster map. It also shows how isolated water bodies that are separated from the river system are not included in the vector data as the thinning algorithm emphasises the production of a linear network. Figure 7 shows the extracted centre line representation of the river network for the entire Niger Delta derived from Sentinel-1 data. The figure reveals a classic deltaic drainage pattern with multiple outlets into the Atlantic Ocean. This pattern is unlike a typical dendritic hydrological catchment with all tributaries draining into one main channel, then into a larger body of water. Here we have a complex network of distributary channels typical of deltaic systems.

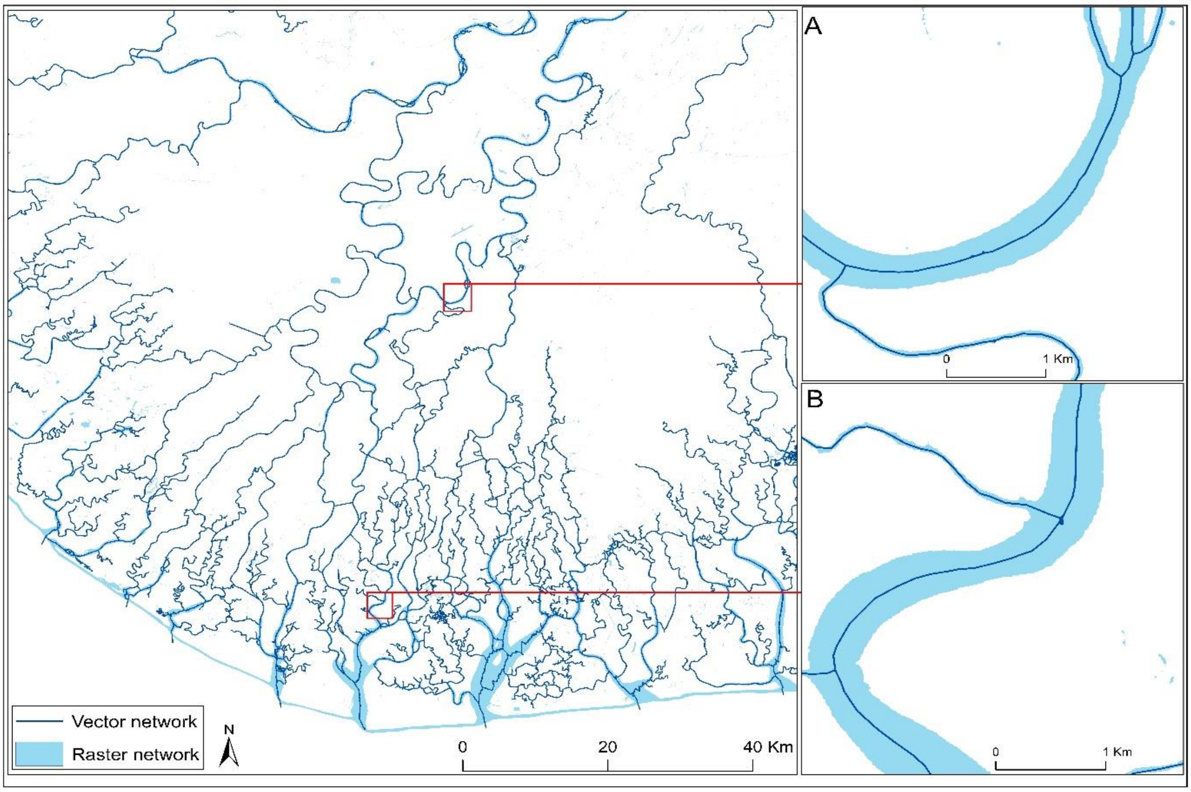

Fig.6. River centrelines overlaid on the raster river data produced from Sentinel-1 data. Inset maps A and B highlight the detail of the raster thinning and river centreline extraction processes.

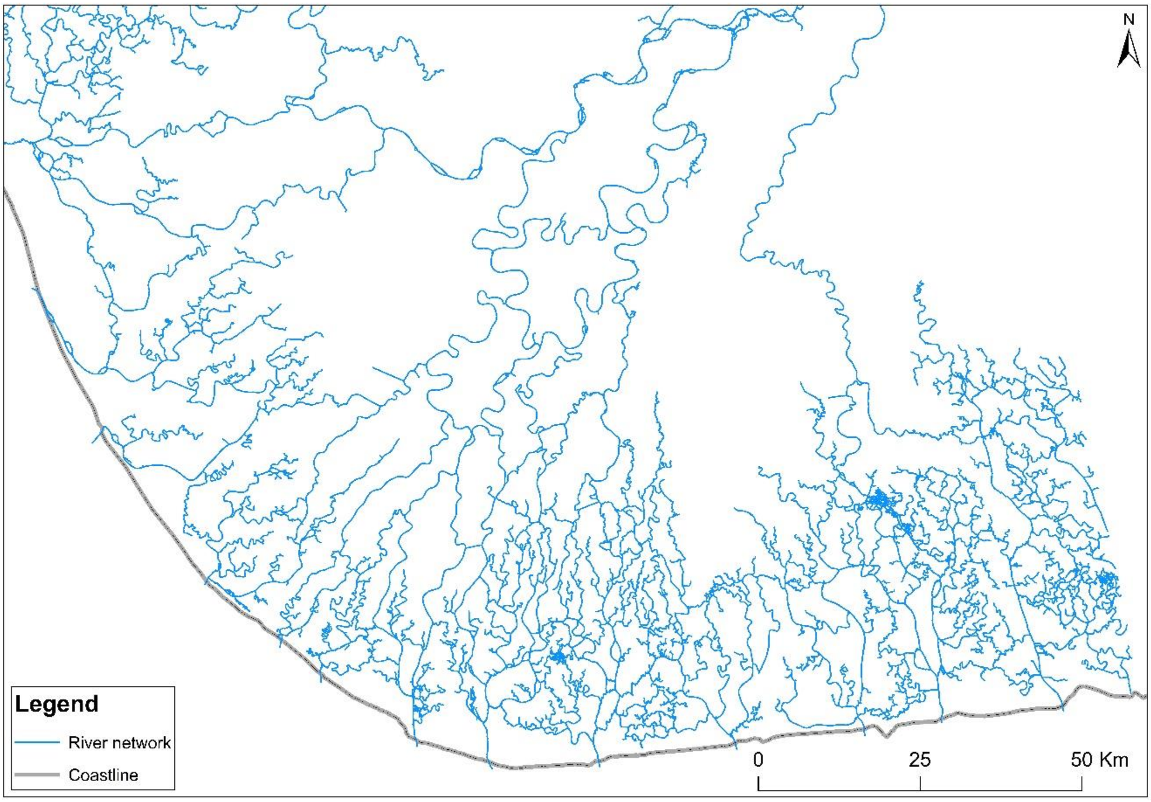

Fig.7. Extracted vector-based river centreline network for the entire delta.

3.2.2 Vector-based accuracy assessment

Figure 8 shows the extent to which the river centre line networks derived from Sentinel-1 and the comparator data sets agree with the reference data. Figures 8B - D show that the networks derived from the comparator data have significant limitations in terms of their completeness and positional accuracy relative to the reference data. This confirms that the higher resolution Sentinel-1 data produces a network that has the closest correspondence with the reference data. This is quantified in Table 2 which shows the results of the vector-based accuracy assessment and demonstrates the superiority of the Sentinel-derived network in terms of completeness. Importantly, delineation of 1st order streams from Sentinel-1 is more than twice as effective as the next-best performing USGS-derived river network. In terms of positional accuracy, Table 3 shows that in all three sections of the network analysed for accuracy, the Sentinel-derived network outperforms all other data sources. It is likely that the superior results for completeness and positional accuracy generated by the Sentinel-derived network result from the higher spatial resolution of the original imagery relative to comparator data sets.

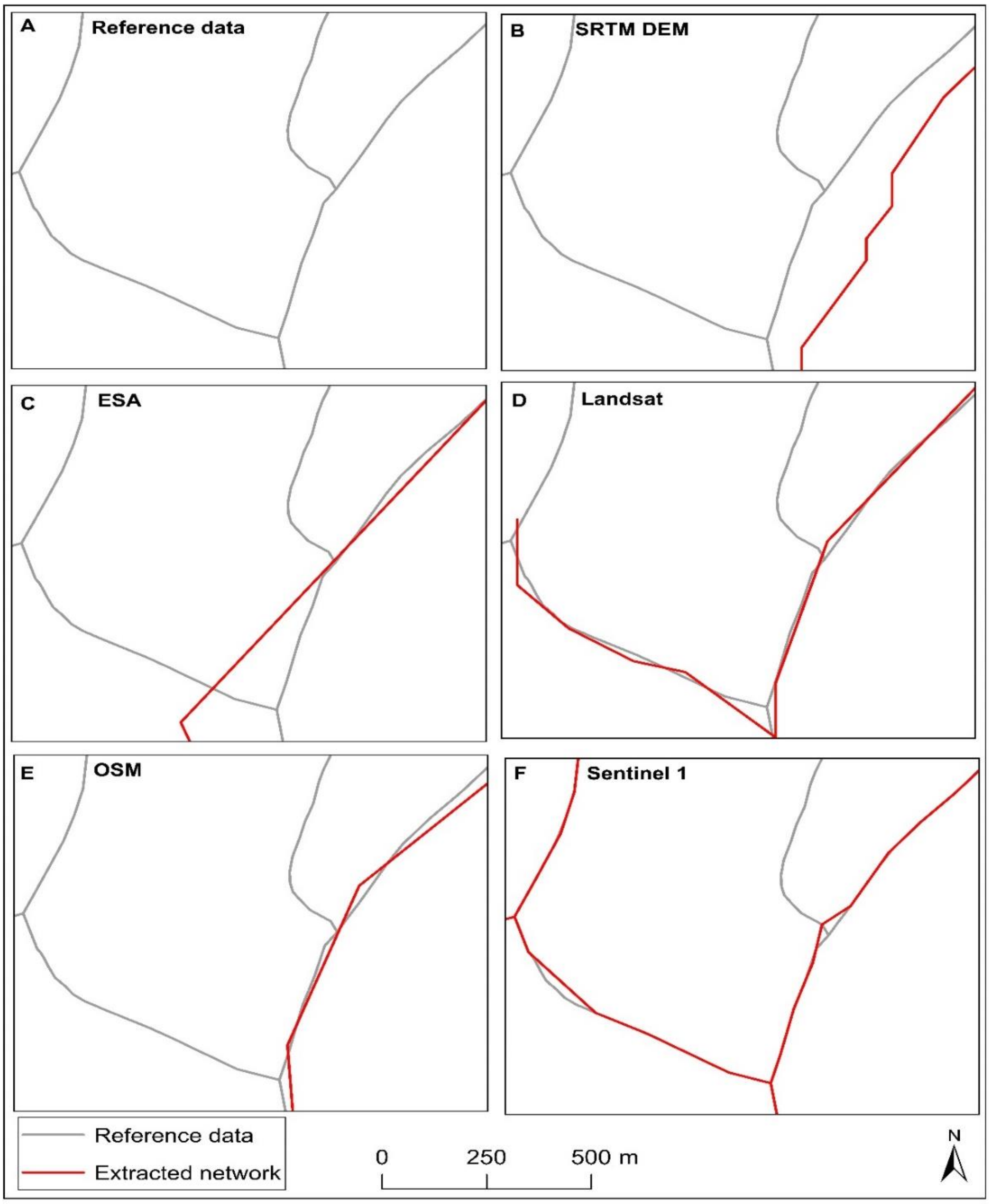

Fig.8. A sample of the river network used to show the reference network data, networks derived from the comparator data sets (SRTM DEM, ESA, USGS and OSM) and the network derived

from Sentinel-1 data. The grey lines shown in all plots are the reference river centrelines which were used for the accuracy assessment.

Table 2.

Results of the network completeness assessment, showing the percentage of the reference network captured by the networks derived from Sentinel-1 and comparator data, for different stream orders and overall.

Data	**3rd order**	**2nd order**	**1st order**	**Overall %**
Sentinel-1	95	76	45	70
USGS	83	46	20	47
ESA data	54	13	2	14
DEM	81	40	15	42
OSM	10	-	-	3

Table 3.

Results of the positional accuracy assessment, showing the percentage of the networks derived from Sentinel-1 and comparator data laying within varied sizes of buffers from the reference network, for three sample sections of the network and on average.

Data	**1st Section**			**2nd Section**			**3rd Section**			**Average %**		
Buffer size	**30m**	**20m**	**10m**	**30m**	**20m**	**10m**	**30m**	**20m**	**10m**	**30m**	**20m**	**10m**
Sentinel-1	81	72	50	98	95	77	100	93	75	93	87	67
USGS	81	60	30	87	70	37	91	78	44	89	69	37
ESA data	14	11	5	17	13	8	26	17	9	19	14	7
OSM	60	47	32	49	35	20	27	17	9	45	33	20
DEM	4	3	1	8	5	6	13	10	7	16	6	5

3.2.3 Case study: application of the geometric river network product to oil pollution dispersal.

Figure 9 shows an example application of the geometric river network in the Niger Delta. This network is topologically structured and comprises edges with attributes such as flow direction and junctions which define connectivity rules between edges. It shows the potential pathway of oil released into the river network from a known point source of crude oil pollution from a broken pipeline and routes pollutants will flow through to the ocean, contingent on network connectivity and flow direction. This example is intended to demonstrate the functionality of the network in permitting a flow routing analysis, rather than a depicting the actual spread of oil from this spill event. While the figure represents a potential route and maximum spread from the source to the ocean sink, the actual spread will depend on a number of factors such as river discharge and rates of oil emulsification and dispersion. Accounting for these additional factors requires a more sophisticated model, which is being developed in our ongoing work, but the river network product developed here provides a spatial framework for defining the key flow pathways in rivers which enable the long distance dissemination of oil pollution in the Niger Delta.

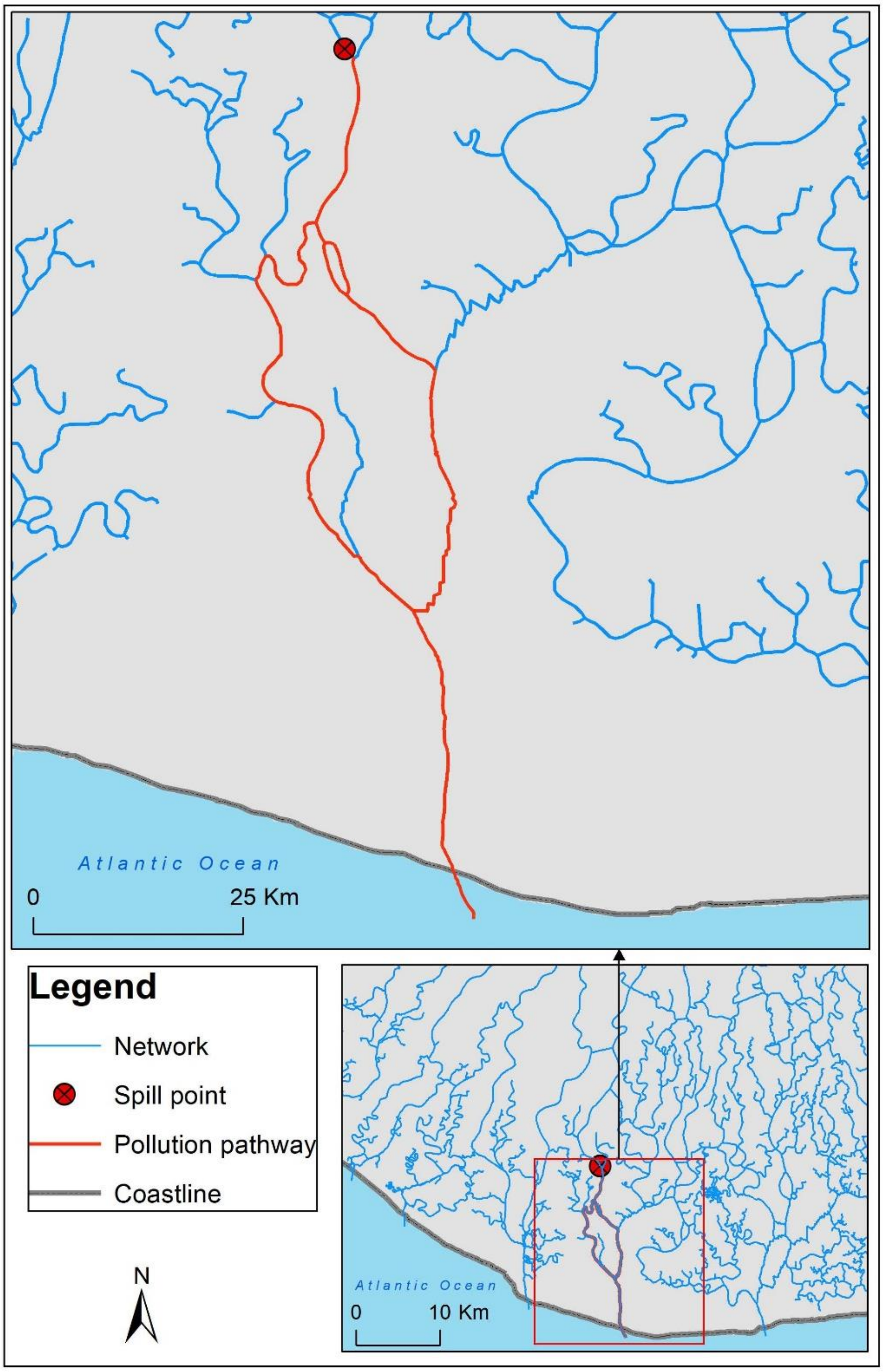

Fig.9. Tracing the potential pathway of oil released from a spill using the extracted river network based on connectivity and attributed flow direction.

4. Discussion

4.1. Unsupervised classification of Sentinel-1 data for water body delineation

As the results demonstrate, the application of unsupervised classification to Sentinel-1 data was effective for mapping water bodies in the study area. This accords with previous work which has found that the application of unsupervised classification to satellite data is an objective, fast and repeatable method of water body delineation (Ogilvie et al., 2015). Unsupervised classification, especially for distinct spectral classes such as water, has been reported to outperform supervised classification or simple thresholding approaches (Zeng et al., 2015). The shortcomings of supervised classification and thresholding in this instance are likely to be associated with the time costs and user subjectivity introduced in selecting training data or appropriate threshold values (Yang et al., 2014; Zeng et al., 2015). The implication is that unsupervised classification is more efficient and accurate.

The k-means unsupervised classification algorithm used in the present study further enhances the robustness of the procedures (Ogilvie et al., 2015; Capó et al, 2017). This is because the algorithm is effective for carrying out segmentation in solving clustering problems (Shah et al., 2011) and because class clustering is performed without prior knowledge of relationships (Tzortzis and Likas, 2014). This is emphasised by the generally high user's accuracy of the Sentinel-1 image classification as shown in Table 1. This suggests that, for anywhere classified as a water body using this algorithm, there is 89% confidence that it is water in the field, meaning that resource managers can be sure of the accuracy of the product (Kennedy et al., 2009).

The time series of Sentinel-1 images used in this study enabled the differentiation of permanent and transient water bodies, in a similar fashion to the use of a MODIS time series by Ogilvie et al. (2015). As shown in Figure 3, the Niger Delta contains a complex network of rivers, creeks, lakes and ponds and flooded areas. Identifying what is permanent and ephemeral is therefore important, particularly for determining the hydrological dynamics of the area during extreme events. Analysis of persistence provides an effective means of mapping permanent water bodies (Figure 4). This type of output is especially important in applications that require only permanent channels, such as for navigation. These data also provide a more effective input for the process of extracting a vector-based representation of the river system, as a connected geometric network of permanent channels.

4.2. River network extraction, topology building and attribution

Vectorization of the classified outputs ensures network data is available in vector formats to accommodate wide-ranging applications (Webster et al., 2016). Figure 7 shows the entire extent of the river network that has been delineated in this study. Automation of the river delineation process can ensure high levels of accuracy and consistency relative to traditional cartographic approaches (Maderal et al., 2016; Yang et al., 2014; Zeng et al., 2015) and the awareness that, in this study, the input data for the delineation was accurately classified, gives further confidence in the network data set. However, it is acknowledged that the river network produced in this study has some limitations. This is illustrated in Table 3, where although Sentinel-1 presents the best results for network delineation in comparison to existing freely available data sets, it cannot resolve all of the first order streams. This is because some of the individual creeks are less than 10m in width, and in some cases no more than 3m wide (Emmanuel and Onyema, 2007). Thus, the 10m spatial resolution of the Sentinel-1 data, combined with tree canopies wholly or partially covering narrow creeks, can limit the ability to delineate the finest features of the river system in the delta.

Although river delineation is an appropriate step, building a geometric network from the output enables more sophisticated forms of analysis. Most applications employing the use of hydrological networks usually require topological information such as flow direction and connectivity rules (Sindhu et al., 2015). As shown in Figure 7, this study was able to produce a geometric river network for the entire study area. The example application demonstrated how the network could then be used for flow routing and assessment of the spread of oil pollution, which is important in the context of the Niger Delta. The river network data will enable future detailed source-pathway-receptor modelling to be carried out to determine the fate of oil spilt as a result of sabotage or operator error (Obida et al., 2018) and similar approaches would be more widely applicable for diverse forms of pollution in other countries. Moreover, many communities in the delta are not connected to the road network, with access only by boats using the river system. Hence, the river network data produced in this study holds considerable potential for assisting in planning more effective (river-based) transportation schemes to support the many isolated and vulnerable communities. There is a pressing need for such applications of river network data in many developing countries.

4.3. Mapping accuracy assessment and comparison framework

Both raster and vector methods of accuracy assessment indicate that the Sentinel-derived products outperform comparator data sets (Tables 2,3,4). Although the Sentinel-based method delineated a substantial proportion of the network, smaller channels were less well discriminated. The systematic methods used in this study for assessing the accuracy of the extracted river centre line ensures consistency. The superior performance of the Sentinel-based method can likely be explained by the higher spatial resolution of the source imagery compared to the comparator data sets and the better discrimination of water bodies achieved by SAR sensing compared to optical sensing (Sabel et al., 2012).

Relatively little data on rivers has been contributed to OSM in the Niger Delta. Lack of OSM content in this region may be explained by the largely rural setting and lack of access to computing hardware and the internet in this region, and a lack of awareness of open-source geospatial technologies like OSM. This accords with studies evaluating the quality of OSM data which revealed substantially greater amounts and detail of digitized data in urban areas compared to remote rural areas (Bittner, 2017; Graham et al., 2015; Neis et al., 2013). To overcome such limitations with user-generated data, the river network data extracted from Sentinel-1 could potentially be fed into OSM to provide better coverage for regions of the world that are less well mapped.

Overall the open access policy for Sentinel-1 data, together with the improved temporal and spatial resolution, constitutes a step change in data supply for resource managers, particularly in developing countries where access to high quality spatial data is limited. The geometric river network that has been generated from Sentinel-1 data in this study opens up opportunities for sophisticated forms of spatial analysis for regions where spatial data is deficient or absent. Therefore, the outputs from this research such as the raster and vector data sets can potentially be made publicly available on sites such as OSM and provided to the Nigeria Hydrological Services Agency, at their request.

5. Conclusion

In this study we demonstrated the capability of using Sentinel-1 data to map a complex river network. This network was assessed for data completeness (length) and positional accuracy (overlap) against a manually digitised reference network. The same accuracy assessment process was conducted for networks derived from the USGS and ESA global water body products, citizen science derived OSM data, and an SRTM DEM. This analysis showed that the network derived from Sentinel-1 is more complete and positionally accurate than those derived from comparator products. Moreover, the topologically-structured geometric river network contains critical information such as flow direction and connectivity rules which permit a range of applications that rely on calculations of flow routes through the system. The open access policy for Sentinel-1 data combined with the straightforward and systematic analytical methods developed in this study open up the opportunity of supplying river network data to the many other regions of the world where such data are out of date, deficient or absent. Consequently, this approach has the potential to generate a step change in the capability of natural resource managers, hydrologist, researchers and government agencies to enhance their workflow and raise their effectiveness in planning and management.

References

Ardhuin, F., Stopa, J., Chapron, B., Collard, F., Smith, M., Thomson, J., Doble, M., Blomquist, B., Persson, O., Collins, C.O., Wadhams, P., 2017. Measuring ocean waves in sea ice using SAR imagery: A quasi-deterministic approach evaluated with Sentinel-1 and in situ data. Remote Sens. Environ. 189, 211–222. https://doi.org/10.1016/j.rse.2016.11.024

Bittner, C., 2017. Diversity in volunteered geographic information: comparing OpenStreetMap and Wikimapia in Jerusalem. GeoJournal 82, 887–906. https://doi.org/10.1007/s10708-016-9721-3

Bolanos, S., Stiff, D., Brisco, B., Pietroniro, A., 2016. Operational surface water detection and monitoring using Radarsat 2. Remote Sens. 8. https://doi.org/10.3390/rs8040285

Capó, M., Pérez, A., Lozano, J.A., 2017. An efficient approximation to the K-means clustering for massive data. Knowledge-Based Syst. 117, 56–69. https://doi.org/10.1016/j.knosys.2016.06.031

Castronova, A.M., Goodall, J.L., 2014. A hierarchical network-based algorithm for multi-scale watershed delineation. Comput. Geosci. 72, 156–166. https://doi.org/10.1016/j.cageo.2014.07.014

Cho, H.-C., Slatton, K.C., Krekeler, C.R., Cheung, S., Clint Slatton, K., 2011. International Journal of Remote Sensing Morphology-based approaches for detecting stream channels from ALSM data Morphology-based approaches for detecting stream channels from ALSM data. Int. J. Remote Sens. 32, 9571–9597. https://doi.org/10.1080/01431161.2011.566896

Domeneghetti, A., Tarpanelli, A., Brocca, L., Barbetta, S., Moramarco, T., Castellarin, A., Brath, A., 2014. The use of remote sensing-derived water surface data for hydraulic model calibration. Remote Sens. Environ. 149, 130–141. https://doi.org/10.1016/j.rse.2014.04.007

Ekeu-Wei, I.T. and Blackburn, G.A., 2018. Applications of Open-Access Remotely Sensed Data for Flood Modelling and Mapping in Developing Regions. Hydrology. https://doi.org/10.3390/hydrology5030039

Emmanuel, B.E., Onyema, I.C., 2007. The Plankton and Fishes of a Tropical Creek in South-Western Nigeria. Turkish J. Fish. Aquat. Sci. 113, 105–113.

Felipe De Almeida Furtado, L., Sanna, T., Silva, F., Márcia, E., De, L., Novo, M., 2016. Dual-season and full-polarimetric C band SAR assessment for vegetation mapping in the Amazon várzea wetlands. Remote Sens. Environ. 174, 212–222. https://doi.org/10.1016/j.rse.2015.12.013

Feyisa, G.L., Meilby, H., Fensholt, R., Proud, S.R., 2014. Automated Water Extraction Index: A new technique for surface water mapping using Landsat imagery. Remote Sens. Environ. 140, 23–35. https://doi.org/10.1016/j.rse.2013.08.029

Fu, B., Wang, Y., Campbell, A., Li, Y., Zhang, B., Yin, S., Xing, Z., Jin, X., 2017. Comparison of object-based and pixel-based Random Forest algorithm for wetland vegetation mapping using high spatial resolution GF-1 and SAR data. Ecol. Indic. 73, 105–117. https://doi.org/10.1016/j.ecolind.2016.09.029

Garneau, C., Sauvage, S., Sánchez-Pérez, J.M., Lofts, S., Brito, D., Neves, R., Probst, A., 2017. Modelling trace metal transfer in large rivers under dynamic hydrology: A coupled hydrodynamic and chemical equilibrium model. Environ. Model. Softw. 89, 77–96. https://doi.org/10.1016/j.envsoft.2016.11.018

Goodchild &, M.F., Hunter, G.J., 1997. A simple positional accuracy measure for linear features. Int. J. Geogr. Inf. Sci. 11, 299–306. https://doi.org/10.1080/136588197242419

Goodchild, M., 2007. How good is Volunteered Geographical Information? A comparative study of OpenStreetMap and Ordnance Survey datasets.

Graham, M., De Sabbata, S., Zook, M.A., 2015. Towards a study of information geographies: (im)mutable augmentations and a mapping of the geographies of information. Geo Geogr. Environ. 2, 88–105. https://doi.org/10.1002/geo2.8

Gülgen, F., 2017. Geocarto International A stream ordering approach based on network analysis operations. Geocarto Int. 32, 322–333. https://doi.org/10.1080/10106049.2016.1140821

Haas, J., Ban, Y., 2017. Sentinel-1A SAR and sentinel-2A MSI data fusion for urban ecosystem service mapping. Remote Sens. Appl. Soc. Environ. 8, 41–53. https://doi.org/10.1016/j.rsase.2017.07.006

Haddeland, I., Heinke, J., Biemans, H., Eisner, S., Flörke, M., Hanasaki, N., Konzmann, M., Ludwig, F., Masaki, Y., Schewe, J., Stacke, T., Tessler, Z.D., Wada, Y., Wisser, D., 2014. Global water resources affected by human interventions and climate change. Proc. Natl. Acad. Sci. U. S. A. https://doi.org/10.1073/pnas.1222475110

Haklay, M., 2010. How good is volunteered geographical information? A comparative study of OpenStreetMap and ordnance survey datasets. Environ. Plan. B Plan. Des. https://doi.org/10.1068/b35097

Hamada, Y., O'Connor, B.L., Orr, A.B., Wuthrich, K.K., 2016. Mapping ephemeral stream networks in desert environments using very-high-spatial-resolution multispectral remote sensing. J. Arid Environ. 130, 40–48. https://doi.org/10.1016/j.jaridenv.2016.03.005

Imperatore, P., Azar, R., Calo, F., Stroppiana, D., Brivio, P.A., Lanari, R., Pepe, A., 2017. Effect of the Vegetation Fire on Backscattering: An Investigation Based on Sentinel-1 Observations. IEEE J. Sel. Top. Appl. Earth Obs. Remote Sens. 10, 4478–4492. https://doi.org/10.1109/JSTARS.2017.2717039

Isikdogan, F., Bovik, A., Passalacqua, P., 2017. RivaMap: An automated river analysis and mapping engine. Remote Sens. Environ. 202, 88–97. https://doi.org/10.1016/j.rse.2017.03.044

Jain, A.K., 2010. Data clustering: 50 years beyond K-means. Pattern Recognit. Lett. 31, 651–666. https://doi.org/10.1016/J.PATREC.2009.09.011

Jiang, Y., 2011. GIS stream network analysis for Huaihe River Basin of China. Procedia Environ. Sci. 10, 1553–1558. https://doi.org/10.1016/j.proenv.2011.09.247

Kadafa, A.A., 2012. Oil Exploration and Spillage in the Niger Delta of Nigeria. Civ. Environ. Res. 2, 2222–2863.

Kennedy, R.E., Townsend, P.A., Gross, J.E., Cohen, W.B., Bolstad, P., Wang, Y.Q., Adams, P., 2009. Remote sensing change detection tools for natural resource managers: Understanding concepts and tradeoffs in the design of landscape monitoring projects. Remote Sens. Environ. 113, 1382–1396. https://doi.org/10.1016/j.rse.2008.07.018

Khan, A., Richards, K.S., Parker, G.T., Mcrobie, A., Mukhopadhyay, B., 2014. How large is the Upper Indus Basin? The pitfalls of auto-delineation using DEMs. J. Hydrol. https://doi.org/10.1016/j.jhydrol.2013.11.028

Khandelwal, A., Karpatne, A., Marlier, M.E., Kim, J., Lettenmaier, D.P., Kumar, V., 2017. An approach for global monitoring of surface water extent variations in reservoirs using MODIS data. Remote Sens. Environ. 202, 113–128.

https://doi.org/10.1016/j.rse.2017.05.039

Kim, D., Muste, M., Merwade, V., 2015. A GIS-based relational data model for multi-dimensional representation of river hydrodynamics and morphodynamics. Environ. Model. Softw. 65, 79–93. https://doi.org/10.1016/j.envsoft.2014.12.002

Kumar, B., Patra, K.C., Lakshmi, V., 2017. Error in digital network and basin area delineation using d8 method: A case study in a sub-basin of the Ganga. J. Geol. Soc. India 89, 65–70. https://doi.org/10.1007/s12594-017-0559-1

Lashermes, B., Foufoula-Georgiou, E., Dietrich, W.E., 2007. Channel network extraction from high resolution topography using wavelets. Geophys. Res. Lett 34, 23–27. https://doi.org/10.1029/2007GL031140

Li, J., Wong, D.W.S., 2010. Effects of DEM sources on hydrologic applications. Comput. Environ. Urban Syst. 34, 251–261. https://doi.org/10.1016/j.compenvurbsys.2009.11.002

Maderal, E.N., Valcarcel, N., Delgado, J., Sevilla, C., Ojeda, J.C., 2016. Automatic river network extraction from LiDAR data. Int. Arch. Photogramm. Remote Sens. Spat. Inf. Sci. - ISPRS Arch. 41, 365–372. https://doi.org/10.5194/isprsarchives-XLI-B8-365-2016

Malenovský, Z., Rott, H., Cihlar, J., Schaepman, M.E., García-Santos, G., Fernandes, R., 2012. Sentinels for science: Potential of Sentinel-1, -2, and -3 missions for scientific observations of ocean, cryosphere, and land. Remote Sens. Environ. 120, 91–101. https://doi.org/10.1016/j.rse.2011.09.026

Miranda, N., Meadows, P.J., Pilgrim, A., Piantanida, R., Recchia, A., Giudici, D., Small, D., Schubert, A., 2016. Sentinel -1B Preliminary Results Obtained During the Orbit

Acquisition Phase [Work in Progress]. Procedia Comput. Sci. 100, 1313–1318. https://doi.org/10.1016/j.procs.2016.09.247

Misra, A., Balaji, R., 2017. Simple Approaches to Oil Spill Detection Using Sentinel Application Platform (SNAP)-Ocean Application Tools and Texture Analysis: A Comparative Study. J. Indian Soc. Remote Sens. 1–11. https://doi.org/10.1007/s12524-016-0658-2

Neis, P., Zielstra, D., Zipf, A., 2013. Comparison of Volunteered Geographic Information Data Contributions and Community Development for Selected World Regions. Futur. Internet 5, 282–300. https://doi.org/10.3390/fi5020282

NHSA, 2014. 2014 Flood outlook for Nigeria [WWW Document]. URL https://docplayer.net/50853781-Nigeria-hydrological-services-agency-2014-flood-outlook-for-nigeria-foreword-honourable-minister-federal-ministry-of-water-resources.html

Obida, C.B., Alan Blackburn, G., Duncan Whyatt, J., Semple, K.T., 2018. Quantifying the exposure of humans and the environment to oil pollution in the Niger Delta using advanced geostatistical techniques. Environ. Int. 111, 32–42. https://doi.org/10.1016/j.envint.2017.11.009

Ogilvie, A., Belaud, G., Delenne, C., Bailly, J.-S., Bader, J.-C., Oleksiak, A., Ferry, L., Martin, D., 2015. Decadal monitoring of the Niger Inner Delta flood dynamics using MODIS optical data. J. Hydrol. 523, 368–383. https://doi.org/10.1016/j.jhydrol.2015.01.036

Passalacqua, P., Belmont, P., Foufoula-Georgiou, E., 2012. Automatic geomorphic feature extraction from lidar in flat and engineered landscapes. Water Resour. Res 48, 3528. https://doi.org/10.1029/2011WR010958

Rahman, M.M., Arya, D.S., Goel, N.K., 2010. Limitation of 90 m SRTM DEM in drainage network delineation using D8 method—a case study in flat terrain of Bangladesh. Appl Geomat 2, 49–58. https://doi.org/10.1007/s12518-010-0020-2

Rahman, M.R., Thakur, P.K., 2017. Detecting, mapping and analysing of flood water propagation using synthetic aperture radar (SAR) satellite data and GIS: A case study from the Kendrapara District of Orissa State of India. Egypt. J. Remote Sens. Sp. Sci. https://doi.org/10.1016/j.ejrs.2017.10.002

Sabel, D., Bartalis, Z., Wagner, W., Doubkova, M., Klein, J.-P., 2012. Development of a Global Backscatter Model in support to the Sentinel-1 mission design. Remote Sens. Environ. 120, 102–112. https://doi.org/10.1016/j.rse.2011.09.028

Senay, G.B., Schauer, M., Friedrichs, M., Velpuri, N.M., Singh, R.K., 2017. Satellite-based water use dynamics using historical Landsat data (1984–2014) in the southwestern United States. Remote Sens. Environ. 202, 98–112. https://doi.org/10.1016/j.rse.2017.05.005

Shah, V., Choudhary, A., Tewari, K., 2011. River extraction from satellite image. Int. J. Comput. Sci. Issues Volume 8, 386–391.

Sindhu, D., Sadashivappa, Ravikumar, A.S., Shivakumar, B.L., 2015. Quantitative Analysis of Catchment Using Remote Sensing and Geographic Information System. Aquat. Procedia 4, 1421–1428. https://doi.org/10.1016/j.aqpro.2015.02.184

Sowter, A., Bin Che Amat, M., Cigna, F., Marsh, S., Athab, A., Alshammari, L., 2016. Mexico City land subsidence in 2014–2015 with Sentinel-1 IW TOPS: Results using the Intermittent SBAS (ISBAS) technique. Int. J. Appl. Earth Obs. Geoinf. 52, 230–242. https://doi.org/10.1016/j.jag.2016.06.015

Tzortzis, G., Likas, A., 2014. The MinMax k-Means clustering algorithm. Pattern Recognit. 47, 2505–2516. https://doi.org/10.1016/J.PATCOG.2014.01.015

UNEP, 2011. Environmental Assessment of Ogoniland.

Veloso, A., Mermoz, S., Bouvet, A., Le Toan, T., Planells, M., Dejoux, J.-F., Ceschia, E., 2017. Understanding the temporal behavior of crops using Sentinel-1 and Sentinel-2-like data for agricultural applications. Remote Sens. Environ. J. https://doi.org/10.1016/j.rse.2017.07.015

Vimal, S., Kumar, D.N., Jaya, I., 2012. Extraction of Drainage Pattern from ASTER and SRTM Data for a River Basin using GIS Tools. Int. Conf. Environ. Energy Biotechnol. 33, 120–124.

Webster, K., Arroyo-Mora, J.P., Coomes, O.T., Takasaki, Y., Abizaid, C., 2016. A cost path and network analysis methodology to calculate distances along a complex river network in the Peruvian Amazon. Appl. Geogr. 73, 13–25. https://doi.org/10.1016/j.apgeog.2016.05.008

Yang, K., Li, M., Liu, Y., Cheng, L., Duan, Y., Zhou, M., 2014. River delineation from remotely sensed imagery using a multi-scale classification approach. J. Sel. Top. Appl. earth Obs. Remote Sens. 7, 4726–4737.

Zeng, C., Bird, S., Luce, J.J., Wang, J., 2015. A natural-rule-based-connection (NRBC) method for river network extraction from high-resolution imagery. Remote Sens. 7, 14055–14078. https://doi.org/10.3390/rs71014055

Zhang, M., Li, Z., Tian, B., Zhou, J., Tang, P., 2016. The backscattering characteristics of wetland vegetation and water-level changes detection using multi-mode SAR: A case study. Int. J. Appl. Earth Obs. Geoinf. 45, 1–13.

https://doi.org/10.1016/j.jag.2015.10.001

https://scihub.copernicus.eu/dhus/

https://landcover.usgs.gov/glc/WaterDescriptionAndDownloads.php

https://www.esa-landcover-cci.org/?q=node/162

https://www.openstreetmap.org/export#map=10/4.7612/6.7387

https://earthexplorer.usgs.gov/

https://www.openstreetmap.org/#map=10/4.7612/6.7387